OXYGEN INFLUENCE ON ESTONIAN KUKERSITE OIL SHALE DEVOLATILIZATION AND CHAR COMBUSTION

LAURI LOO[*], BIRGIT MAATEN, DMITRI NESHUMAYEV, ALAR KONIST

Department of Energy Technology, Tallinn University of Technology, Ehitajate tee 5, 19086 Tallinn, Estonia

Abstract. *This work investigated the kinetic parameters of the thermal decomposition of Estonian kukersite oil shale (OS) organic part in air atmospheres at various oxygen-nitrogen ratios. During oil shale combustion, two combustion phases were recognized but could not be separated. Thermogravimetric analysis (TGA) of oil shale combustion was conducted in nitrogen-based gases at different oxygen concentrations (5–50% O_2) and heating rates (1, 10, 30 and 50 K/min). The authors modeled oil shale devolatilization and char combustion at different oxygen concentrations by using a discrete activation energy model. The process could be described by four parallel independent reactions. The activation energies were 105–134 kJ/mol. The combustion rate was found to be dependent on oxygen partial pressure. The power variables of the oxygen concentration for the reaction models were optimized and compared against a unity base case. Using these data, oil shale devolatilization and char combustion in nitrogen-based environments were modeled.*

Keywords: *oil shale devolatilization, thermogravimetric analysis, oxygen influence, kukersite kerogen, combustion kinetics, parallel reaction model.*

1. Introduction

Oil shale (OS) is a low-grade fossil fuel consisting of kerogen and mineral components. It can be utilized for energy production via pyrolysis or direct combustion. In Estonia, both types of energy conversion technologies are used, and OS is also used in cement production [1]. Approximately 80% of electricity in Estonia is produced from this rock [2–4]. A fundamental study of oil shale combustion kinetics would aid in predicting its combustion behaviour and designing and developing efficient combustion systems.

The properties of oil shale vary depending on different deposit sources. For example, the gross heating value of oil shale on a dry basis ranges from

---

[*] Corresponding author: e-mail *lauri.loo@ttu.ee*

approximately 2.8 to 16.8 MJ/kg. The mineral components of OS may also primarily contain carbonate or clay-based minerals [5]. Similarly, the composition of OS kerogen, an insoluble macromolecular organic matter, differs between deposits from different parts of the world [6]. Accordingly, the thermal decomposition behaviour of oil shales varies.

A review of worldwide OS reserves by Altun et al. [7] indicated enormous energy potential. Thermal engineering experience in Estonia [8–10] has shown that the fluidized bed combustion of OS is the best available technology due to a high process efficiency, low emissions and no requirements for an additional flue gas cleaning system to conventional fly ash removal equipment. Past studies have also shown [11–13] that circulating fluidized bed (CFB) combustion technology is capable of co-combustion, thereby enabling fuel flexibility. The purpose of the present investigation is to provide fundamental parameters necessary for the future development of OS combustion technology.

Our previous study [14] showed that OS combustion is a complex process. At least two overlapping mass loss rate peaks were observed during the combustion of the organic components of OS (i.e. combustion zone, Fig. 1). This implied competing or parallel reactions. Burnham and Braun [15] proposed distributed reactivity models for the kinetic analysis of complex materials. Jamaluddin et al. [16] and Anthony et al. [17] used a similar
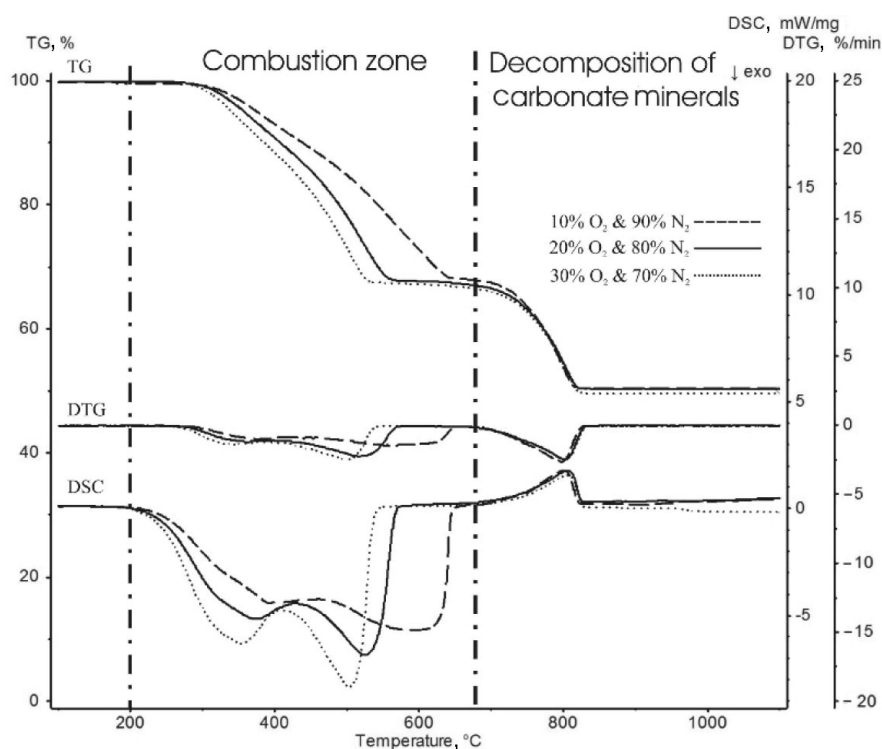

Fig. 1. Thermal decomposition of Estonian kukersite oil shale [14].

approach in describing bituminous coal devolatilization with good results. Sundararaman et al. [18] implemented activation energy distribution methods for kerogen pyrolysis.

Oil shale combustion has been widely studied by researchers worldwide [19–26]. These reports have provided interesting data; however, most combustion experiments were conducted in air. Few studies have investigated the effect of oxygen concentration on combustion. Yörük et al. [27] modeled Estonian oil shale combustion by using the Friedman differential method under different types of atmospheres. Han et al. [25], Liu et al. [28], Li et al. [29] and Bai et al. [30] have explored the influence of oxygen concentration on the combustion processes of solid fuels. We used these reports as starting points for the present analysis. We implemented the distributed activation energy method (DAEM) and examined the effect of oxygen concentration on OS combustion.

Herein we focused on the combustion of organics in OS and the influence of oxygen concentration on the process. The combustion kinetics was studied using thermogravimetric analysis (TGA). A parallel reaction model was employed to simulate the combustion of OS. The effect of oxygen concentration in nitrogen on combustion was investigated.

2. Materials and methods

2.1. Materials

The experiments were conducted with a kukersite OS sample collected from an underground mine in Estonia. The sample used in this study was similar to the one employed by our research group in previous studies [14, 31] to describe OS combustion characteristics, ash formation and sulphur retention during regular and oxy-fuel combustion. The OS sample was dried at 105 °C for three hours, crushed, and passed through a sieve with 1-mm openings. The sample particles median diameter (d_m) was 180 μm and the specific surface area (MBET) was 9.0 m^2/g. The results of elemental and proximate analyses of oil shale and composition of laboratory ash are presented in Table 1.

Table 1. Elemental and proximate analyses of Estonian kukersite oil shale and composition of laboratory ash [14]

Elemental analysis of oil shale, %		Proximate analysis of oil shale		Composition of laboratory ash, %	
H	2.9	$Ash_{815°C}$	47.0%	SiO_2	30.7
C	27.9	Net calorific value	9.08 MJ/kg	FeO_3	4.8
N	0.07	Volatile matter	52.3%	Al_2O_3	6.1
S	1.52	Fixed carbon	0.5%	CaO	39.0
		Moisture	0.2%	MgO	8.7
$S_{sulphate}$	0.07			K_2O	1.8
$S_{sulphide}$	0.96			Na_2O	0.1
$S_{organic}$	0.49				
CO_{2carb}	20.12				

2.2. Equipment and procedures

The authors conducted the thermal analyses on a Netzsch STA 449 F3 Jupiter Simultaneous Thermal Analyzer (TG-DSC/DTA Apparatus). The samples were analysed in Pt/Rh crucibles equipped with removable liners composed of thin-walled Al_2O_3. Approximately 4 mg of the OS sample was used in each experiment. The total gas flow rate during all measurements was 60 ml/min. To ensure that the gas flow was sufficient to maintain stable conditions, a few experiments were conducted under double gas flow. Changing the gas flow did not change the mass loss behaviour of the samples. During TGA, the OS samples were heated at a constant heating rate up to 800 °C. All measurements were obtained in nitrogen-based gases at different oxygen concentrations (5–50% O_2) and heating rates (1, 10, 30 and 50 K/min). The instrument temperature measurement was calibrated with In, Sn, Zn, Al and Au standards. All measurements were performed at least twice for reproducibility. Despite the non-homogeneous nature of the material and the particle size distribution used, good reproducibility was achieved. The maximum deviation of the mass loss rate (DTG) peak was less than 2 K.

2.3. Kinetic model

The initial sample mass was measured at 200 °C for each sample. A complete organic burnout was achieved at temperatures from 460 to 680 °C. The degree of the cumulative combustion reaction was expressed by Equation (1):

$$a = \frac{m_o - m_t}{m_o - m_{bo}},$$
(1)

where α is the extent of conversion; m_o is the initial sample mass, kg; m_{bo} is the sample burnout mass, kg; m_t is the sample mass at time t, kg.

Many studies have explored char oxidation [32–37] and have considered the global reaction rate to follow Equation (2):

$$\frac{d\alpha}{dt} = kf(\alpha) = A\exp\left(-\frac{E}{RT}\right)p_{O_2}^n (1-\alpha),$$
(2)

where α is the extent of conversion; A is the Arrhenius pre-exponential factor, 1/s; E is the activation energy, J/mol; k is the rate constant, 1/s; p_{O_2} is the partial pressure of oxygen, atm; R is the gas constant, J/(mol·K); t is the time, s; T is the temperature, K; n is the exponent of oxygen partial pressure.

Char combustion is a complex process. Typically, the overall process is assumed to be a uniform first-order decomposition. However, the combustion of OS is an even more complex process (Eq. (3)) and further involves devolatilization as well as the combustion of volatiles and char. Herein we

described the process by parallel independent reactions. We further assumed that OS combustible matter consisted of a number of homogeneous species, i.e. $w_1…w_l$. The components were assumed to decompose simultaneously at their respective different rates at different temperatures as follows:

$$OS + [O_2] \xrightarrow{\ k\ } Volatile\,1 + Volatile\,2 + Volatile\,N + ash \qquad (3)$$

The decomposition rate of all combustible species was expressed by the following equation:

$$\frac{d\alpha}{dt} = \sum_{i=1}^{l} A_l \exp\left(-\frac{E_l}{RT}\right) p_{O_2}^{n_l} (w_l - \alpha_l), \qquad (4)$$

where α is the extent of conversion; A is the Arrhenius pre-exponential factor, 1/s; E is the activation energy, J/mol; k is the rate constant, 1/s; l is the number of parallel reactions; n is the exponent of oxygen partial pressure; p_{O_2} is the partial pressure of oxygen, atm; R is the gas constant, J/(mol·K); t is the time, s; T is the temperature, K; w is the weight of the reaction.

With sufficient excess gas flow in the reactor, a constant oxygen partial pressure can be assumed. Therefore, $p_{O_2}^{n}$ can be incorporated into the pre-exponential factor. By using Kinetics2015 software, a discrete activation energy analysis was performed, and the kinetic parameters describing the combustion reaction at a 20% oxygen concentration in nitrogen were obtained. This was used as the base case for examining the influence of oxygen on combustion.

2.4. Evaluation of the power of oxygen partial pressure

The obtained pre-exponential factors were assumed to incorporate the partial pressure of oxygen at the power of n_l. A good model should describe a reaction in the wide range of said pressure. To determine the power of oxygen partial pressure, a number of different methods were used and compared with a base case, i.e. with the exponent of oxygen partial pressure being one.

The root mean square error (RMSE) of all reactions (Eq. (5)) was minimized with a MATLAB algorithm, fmincon. This method provided the minimum average error:

$$RMSE = \frac{\sum_{j=1}^{N_{exp}} \sqrt{\dfrac{\sum_{q=1}^{N_j} \left(\alpha_{j,q}^{obs} - \alpha_{j,q}^{\mathrm{model}} \right)^2}{N_j}}}{N_{exp}} \to \min, \qquad (5)$$

where $\alpha_{j,q}^{obs}$ is the extent of conversion during the experiment j at measured point q; $\alpha_{j,q}^{\mathrm{model}}$ is the modeled extent of conversion j at measured

point q; N_{exp} is the number of experiments; N_j is the number of measured points during the experiment j.

The maximum root square error (MRSE) was minimized (Eq. (6)) to obtain the minimal maximum error:

$$MRSE = \max_{j=1}^{N_{exp}} \left[\max_{q=1}^{N_j} \sqrt{\left(\alpha_{j,q}^{obs} - \alpha_{j,q}^{model} \right)^2} \right] \to \min, \qquad (6)$$

where $\alpha_{j,q}^{obs}$ is the extent of conversion during the experiment j at measured point q; $\alpha_{j,q}^{model}$ is the modeled extent of conversion j at measured point q; N_{exp} is the number of experiments; N_j is the number of measured points during the experiment j.

The mean of the maximum root square error (MMRSE) of different experiments was minimized (Eq. (7)) to obtain the minimal error at any random point:

$$MMRSE = \text{mean}_{j=1}^{N_{exp}} \left[\max_{q=1}^{N_j} \sqrt{\left(\alpha_{j,q}^{obs} - \alpha_{j,q}^{model} \right)^2} \right] \to \min, \qquad (7)$$

where $\alpha_{j,q}^{obs}$ is the extent of conversion during the experiment j at measured point q; $\alpha_{j,q}^{model}$ is the modeled extent of conversion j at measured point q; N_{exp} is the number of experiments; N_j is the number of measured points during the experiment j.

These results were compared and conclusions were drawn.

3. Results and discussion

3.1. The parallel reaction model

The base case for evaluating the kinetic parameters of combustion was the experiment conducted in a near air environment, i.e. 20% O_2 and 80% N_2. The measurement results obtained at different heating rates are shown in Figure 2. As mentioned above, two characteristic peaks were observed on the mass loss rate curve, indicating that at least two parallel reactions occurred. The kinetic parameters were determined and are given in Table 2. The results of the kinetic analyses were compared with the experimental measurements and are shown in Figure 3. The increasing number of parallel reactions decreased the prediction error but increased the complexity of the calculations. Four parallel reactions were found to be sufficient to describe the OS combustion process (RMSE 0.011 and MRSE 0.027 at 50 K/min).

Parallel reaction models have been useful for describing biomass pyrolysis [38, 39]. In these works, each parallel reaction represented one component of the biomass: hemicellulose, cellulose and lignin. The organic component of OS is composed of only one macromolecular component, kerogen. In the current research, the parallel reactions were not considered substitutes for real chemical reactions, but, instead, were used to simplify complex reaction schemes.
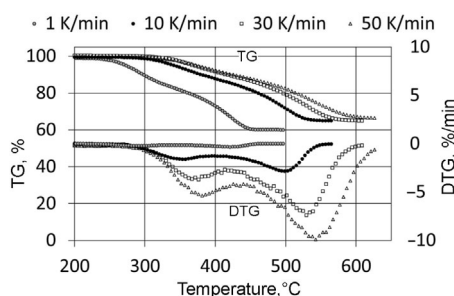
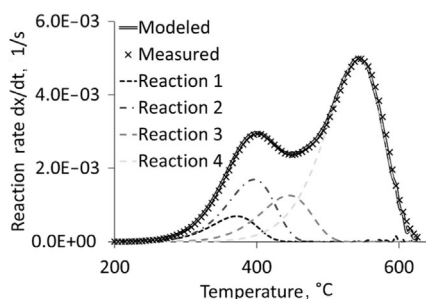Fig. 2. TG-DTG curves of Estonian oil shale in 20% O_2 and 80% N_2 at different heating rates.

Fig. 3. The rate of Estonian oil shale organics combustion at 50 K/min in 20% O_2 and 80% N_2. (The dots represent the measured reaction rate, the dashed lines represent each parallel reaction contributing to the modeled reaction rate described by the solid line.)

Table 2. The kinetic parameters of Estonian oil shale devolatilization and the remaining coke combustion in 20% O_2 and 80% N_2

Reaction number, m	Weight of the reaction, w	Activation energy, E, kJ/mol
1	0.07	104.6
2	0.17	108.8
3	0.14	117.2
4	0.62	133.9

Note: The pre-exponential factor, A, had a fixed value of 7.02E + 06 1/s.

3.2. Evaluation of the power of oxygen partial pressure

We had previously shown that oxygen content and the main gas composition strongly influenced the combustion process [14]. Differences between OS air and oxy-fuel combustion parameters increased at low oxygen levels. While the prior study presented experimental work and observations about the process, neither combustion model nor kinetic parameters were proposed.

The present work examined OS devolatilization and char burnout prediction (Fig. 4), and provided the kinetic parameters of the process (Table 3).

For the base case scenario the power of oxygen partial pressure was chosen one (see Eq. (4)). We used several criteria to determine the best fitting oxygen concentration exponent (see Eqs. (5)–(7)). There were several local but no global optima (see Table 4 and Fig. 5). The best solution was obtained by RMSE and MRSE, and with solution c of 0.52, 0.65, 0.73 and 1.13. The latter resulted in an approximately 13% lower error compared to the base case scenario (Fig. 4). For the base case (a), the results fit better at higher oxygen concentrations, while the optimized solution (c) correlated better with the measured data at lower oxygen concentrations.
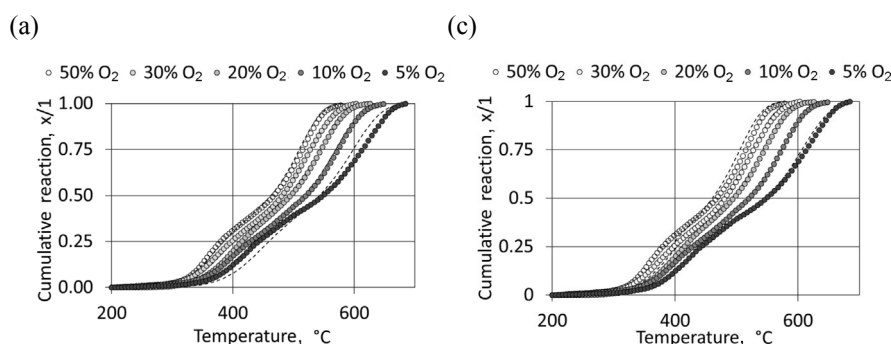
(a)   (c)

Fig. 4. The measured (dots) and modeled (lines) conversions of kerogen in a nitrogen atmosphere when varying O_2 content at a heating rate of 50 K/min. The modeled lines were calculated using unity as a power of oxygen a (1; 1; 1; 1) and optimal oxygen partial pressure exponent c (0.52; 0.65; 0.73; 1.13).

Table 3. The kinetic constants of oil shale combustion for Equation (4) using the optimal solution (c)

Reaction number, m	Weight of the reaction, w	Pre-exponential factor, A, 1/s	Activation energy, E, kJ/mol	Power of oxygen concentration, n
1	0.0691	1.61E + 07	104.6	0.5164
2	0.1735	2.01E + 07	108.8	0.6538
3	0.1392	2.27E + 07	117.2	0.7286
4	0.6181	4.35E + 07	133.9	1.1340

Han et al. [25] investigated the combustion of Huadian OS and found the process to be homogeneous at early stages. However, at high temperatures, the combustion shifted to a heterogeneous stage. The reaction speed of volatiles was assumed independent of oxygen concentration, and the reaction of char was considered proportional to the oxygen partial pressure. These results indicated that the entire combustion process was dependent on

Table 4. Solutions for the optimization of the power of partial pressure of oxygen

	n				RMSE		MRSE		MMRSE	
l	1	2	3	4	Absolute	Relative difference, %	Absolute	Relative difference, %	Absolute	Relative difference, %
w	0.07	0.17	0.14	0.62						
a	1.00	1.00	1.00	1.00	0.0224	0	0.0516	0	0.0769	0
b	0.00	1.00	1.00	1.00	0.0214	−4	0.0496	−4	0.0768	0
c	0.52	0.65	0.73	1.13	0.0196	−13	0.0451	−13	0.0649	−16
d	0.59	0.53	0.94	1.10	0.0199	−11	0.0448	−13	0.0624	−19
e	0.95	0.51	0.82	1.08	0.0201	−10	0.0463	−10	0.0608	−21
f	0.00	0.00	0.00	0.00	0.0844	277	0.1841	257	0.3374	339

Abbreviations and symbols used: RMSE – root mean square error; MRSE – maximum root square error; MMRSE – mean of the maximum root square error; l – number of parallel reactions; w – weight of the reaction; n – exponent of oxygen partial pressure; a, b, c, d, e, f – solutions.
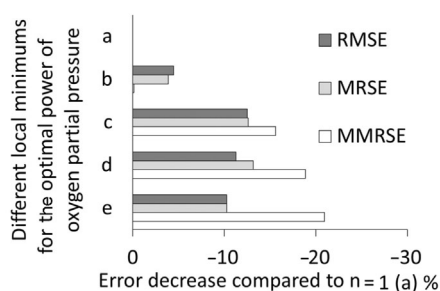

Fig. 5. Comparison of different solutions for a minimal error of oil shale combustion. (Solution f is not displayed because the error is enormous.)

oxygen concentration. Similar conclusions were drawn by Liu et al. [28]. The researchers noticed that oxygen concentration had a weak effect on the ignition of coal and a strong effect on the burnout temperature. Our results confirmed these observations and further correlated the reaction rate with oxygen partial pressure.

The assumptions that OS volatility and char combustion followed the Arrhenius equation and were dependent on oxygen partial pressure seem to have been validated. These assumptions also corresponded with the observation about significant differences of conversion at the end of the reaction and nearly no differences at the start of the combustion process (the oxygen concentration only changed the rate and not the course of the reactions). This study confirmed that combustion followed the same path, i.e. at 5–50% oxygen in nitrogen. Liu et al. [28] conducted combustion experiments with coal at 3.3% oxygen in a nitrogen atmosphere and found that the reactions followed the same path as those conducted at higher oxygen concentrations.

3.3. Burnout time of oil shale

Simplified burnout times were calculated along isotherms to compare the Estonian OS combustion process with those of other fuels (Fig. 6). The differences between fuels were significant at lower temperatures. At higher temperatures, the differences in reaction time decreased. The Estonian OS combustion time was rather short when compared with those of the high quality coals.
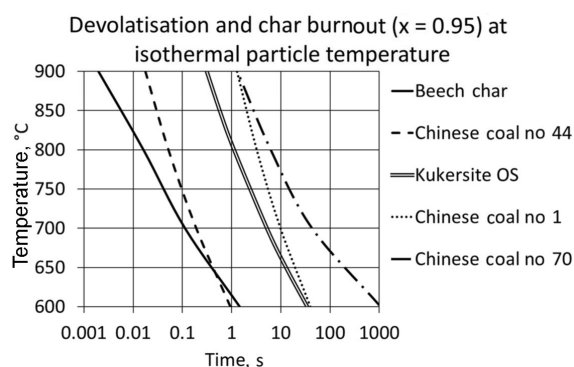

Fig. 6. Devolatilization and the remaining char burnout (x = 0.95) times at isothermal temperatures assuming reaction kinetics-controlled combustion and stable oxygen concentration 20%. The comparisons are based on [40] and [41].

This research only mapped the behaviour of rather small particles (d_m = 180 μm). However, fluidized bed boilers typically use fuel with particle diameters up to 12 mm. Therefore, the influence of the particle size should be further studied to predict fuel behaviour in real combustion systems. Furthermore, the influence of oxygen concentration was mapped for a rather wide range of O_2 concentration in N_2, from 5 to 50%, and the oxygen consumption was neglected. Consumption of oxygen and its diffusion to particles would require further investigation.

4. Conclusions

During oil shale combustion, the recognized combustion phases could not be separated. Thermogravimetric analysis conducted in nitrogen-based gases at different oxygen concentrations was used to simulate oil shale combustion. The authors modeled OS devolatilization and char combustion at different oxygen concentrations by using a discrete activation energy model. The process could be described by four parallel independent reactions. The orders of oxygen concentration for the reactions were optimized. The activation energies were 105–134 kJ/mol and the pre-exponential factors

were 1.6E07–4.4E07 1/s. The optimization of the power of oxygen partial pressure resulted in a 13% decrease in the root mean square error when compared with that for a linear reaction rate dependence on oxygen partial pressure. The best fit was obtained when power variables of oxygen partial pressure for parallel reactions were 0.52, 0.65, 0.73 and 1.13. This study showed that oil shale devolatilization and char combustion rate depended on the oxygen partial pressure. Using this data, OS devolatilization and char combustion could be modeled in nitrogen-based environments.

REFERENCES

1. Soone, J., Doilov, S. Sustainable utilization of oil shale resources and comparison of contemporary technologies used for oil shale processing. *Oil Shale*, 2003, **20**(3), 311–323.
2. Siirde, A. Oil shale – global solution or part of the problem? *Oil Shale,* 2008, **25**(2), 201–202.
3. FE032: *Capacity and Production of Power Plants.* Est. Stat., 2017. www.stat.ee (accessed February 10, 2017).
4. Roos, I., Soosaar, S., Volkova, A., Streimikene, D. Greenhouse gas emission reduction perspectives in the Baltic States in frames of EU energy and climate policy. *Renew. Sust. Energ. Rev.*, 2012, **16**(4), 2133–2146.
5. Dyni, J. R. Geology and resources of some world oil-shale deposits. *Oil Shale*, 2003, **20**(3), 193–252.
6. Vandenbroucke, M., Largeau, C. Kerogen origin, evolution and structure. *Org. Geochem.*, 2007, **38**(5), 719–833.
7. Altun, N ., Hiçyilmaz, C., Hwang, J.-Y., Suat Bağci, A., Kök, M. V. Oil shales in the world and Turkey; reserves, current situation and future prospects: A review. *Oil Shale*, 2006, **23**(3), 211–227.
8. Konist, A., Pihu, T., Neshumayev, D., Siirde, A. Oil shale pulverized firing: boiler efficiency, ash balance and flue gas composition. *Oil Shale*, 2013, **30**(1), 6–18.
9. Pihu, T., Konist, A., Neshumayev, D., Loosaar, J., Siirde, A., Parve, T., Molodtsov, A. Short-term tests on firing oil shale fuel applying low-temperature vortex technology. *Oil Shale*, 2012, **29**(1), 3–17.
10. Plamus, K., Soosaar, S., Ots, A., Neshumayev, D. Firing Estonian oil shale of higher quality in CFB boilers – environmental and economic impact. *Oil Shale*, 2011, **28**(1S), 113–126.
11. Konist, A., Pihu, T., Neshumayev, D., Külaots, I. Low grade fuel – oil shale and biomass co-combustion in CFB boiler. *Oil Shale*, 2013, **30**(2S), 294–304.
12. Pihu, T., Konist, A., Neshumayev, D., Loo, L. Molodtsov, A., Valtsev, A. Full-scale tests on the co-firing of peat and oil shale in an oil shale fired circulating fluidized bed boiler. *Oil Shale* (in the press).
13. Pihu, T., Konist, A., Neshumayev, D., Loo, L., Veinjärv, R. Combustion of Fuel Mixtures in Oil Shale Fired CFBC and PC Boilers. *Presentation at International Oil Shale Symposium 2016,* Tallinn, Estonia, 2016.
14. Loo, L., Maaten, B., Siirde, A., Pihu, T., Konist, A. Experimental analysis of the combustion characteristics of Estonian oil shale in air and oxy-fuel atmospheres. *Fuel Process. Technol.*, 2015, **134**, 317–324.

15. Burnham, A. K., Braun, R. L. Global kinetic analysis of complex materials. *Energ. Fuel.*, 1999, **13**(1), 1–22.

16. Jamaluddin, A. S., Truelove, J. S., Wall, T. F. Modeling of coal devolatilization and its effect on combustion calculations. *Combust. Flame*, 1985, **62**(1), 85–89.

17. Anthony, D. B., Howard, J. B., Hottel, H. C., Meissner, H. P. Rapid devolatilization and hydrogasification of bituminous coal. *Fuel*, 1976, **55**(2), 121–128.

18. Sundararaman, P., Merz, P. H., Mann, R. G. Determination of kerogen activation energy distribution. *Energ. Fuel.*, 1992, **6**(6), 793–803.

19. Kök, M. V., Pamir, M. R. Comparative pyrolysis and combustion kinetics of oil shales. *J. Anal. Appl. Pyrol.*, 2000, **55**(2), 185–194.

20. Kök, M. V., Pokol, G., Keskin, C., Madarász, J., Bagci, S. Combustion characteristics of lignite and oil shale samples by thermal analysis techniques. *J. Therm. Anal. Calorim.*, 2004, **76**(1), 247–254.

21. Kök, M. V., Iscan, A. G. Oil shale kinetics by differential methods. *J. Therm. Anal. Calorim.*, 2007, **88**(3), 657–661.

22. Liu, Q. Q., Han, X. X., Li, Q. Y., Huang, Y. R., Jiang, X. M. TG-DSC analysis of pyrolysis process of two Chinese oil shales. *J. Therm. Anal. Calorim.*, 2014, **116**(1), 511–517.

23. Jiang, X. M., Cui, Z G., Han, X. X., Yu, H. L. Thermogravimetric investigation on combustion characteristics of oil shale and high sulphur coal mixture. *J. Therm. Anal. Calorim.*, 2006, **85**(3), 761–764.

24. Yan, J., Jiang, X., Han, X., Liu, J. A TG–FTIR investigation to the catalytic effect of mineral matrix in oil shale on the pyrolysis and combustion of kerogen. *Fuel*, 2013, **104**, 307–317.

25. Han, X. X., Jiang, X M., Cui, Z. G. Mathematical model of oil shale particle combustion, *Combust. Theor. Model.*, 2006, **10**(1), 145–154.

26. Aboulkas, A., El Harfi, K. Study of the kinetics and mechanisms of thermal decomposition of Moroccan Tarfaya oil shale and its kerogen. *Oil Shale*, 2008, **25**(4), 426–443.

27. Yörük, C. R., Meriste, T., Trikkel, A., Kuusik, R. Oxy-fuel combustion of Estonian oil shale: kinetics and modeling. *Energy Procedia*, 2016, **86**, 124–133.

28. Liu, Y., Wang, C., Che, D. Ignition and kinetics analysis of coal combustion in low oxygen concentration. *Energ. Source. Part A*, 2012, **34**(9), 810–819.

29. Li, Q., Zhao, C., Chen, X., Wu, W., Li, Y. Comparison of pulverized coal combustion in air and in O_2/CO_2 mixtures by thermo-gravimetric analysis. *J. Anal. Appl. Pyrol.*, 2009, **85**(1–2), 521–528.

30. Bai, F., Sun, Y., Liu, Y. Thermogravimetric analysis of Huadian oil shale combustion at different oxygen concentrations. *Energ. Fuel.*, 2016, **30**(6), 4450–4456.

31. Konist, A., Valtsev, A., Loo, L., Pihu, T., Liira, M., Kirsimäe, K. Influence of oxy-fuel combustion of Ca-rich oil shale fuel on carbonate stability and ash composition. *Fuel*, 2015, **139**, 671–677.

32. Goldfarb, J. L., D'Amico, A., Culin, C., Suuberg, E. M., Külaots, I. Oxidation kinetics of oil shale semicokes: reactivity as a function of pyrolysis temperature and shale origin. *Energ. Fuel.*, 2013, **27**, 666–672.

33. Di Blasi, C. Combustion and gasification rates of lignocellulosic chars. *Prog. Energ. Combust.*, 2009, **35**(2), 121–140.

34. Han, X., Kulaots, I., Jiang, X., Suuberg, E. M. Review of oil shale semicoke and its combustion utilization. *Fuel*, 2014, **126**, 143–161.

35. Murphy, J. J., Shaddix, C. R. Combustion kinetics of coal chars in oxygen-enriched environments. *Combust. Flame*, 2006, **144**, 710–729.

36. Beeston, G. Kinetics of coal combustion: the influence of oxygen concentration on the burning-out times of single particles. *J. Phys. Chem-US*, 1963, **67**(6), 1349–1355.

37. Bews, I. M., Hayhurst, A. N., Richardson, S. M., Taylor, S. G. The order, Arrhenius parameters, and mechanism of the reaction between gaseous oxygen and solid carbon. *Combust. Flame*, 2001, **124**(1–2), 231–245.

38. Vamvuka, D., Kakaras, E., Kastanaki, E., Grammelis, P. Pyrolysis characteristics and kinetics of biomass residuals mixtures with lignite. *Fuel*, 2003, **82**(15–17), 1949–1960.

39. Sfakiotakis, S., Vamvuka, D. Development of a modified independent parallel reactions kinetic model and comparison with the distributed activation energy model for the pyrolysis of a wide variety of biomass fuels. *Bioresource Technol.*, 2015, **197**, 434–442.

40. Yang, J., Zhang, X., Zhao, H., Shen, L. Non-linear relationship between combustion kinetic parameters and coal quality. *J. Zhejiang Univ. Sci. A*, 2012, **13**(5), 344–352.

41. Branca, C., Di Blasi, Global kinetics of wood char devolatilization and combustion. *Energ. Fuel.,* 2003, **17**(6), 1609–1615.